

# Replica symmetric evaluation of the information transfer in a two-layer network in presence of continuous and discrete stimuli

Valeria Del Prete and Alessandro Treves

*SISSA, Programme in Neuroscience, via Beirut 4, Trieste, Italy*

## Abstract

In a previous report we have evaluated analytically the mutual information between the firing rates of  $N$  independent units and a set of multi-dimensional continuous+discrete stimuli, for a finite population size and in the limit of large noise. Here, we extend the analysis to the case of two interconnected populations, where input units activate output ones via gaussian weights and a threshold linear transfer function. We evaluate the information carried by a population of  $M$  output units, again about continuous+discrete correlates. The mutual information is evaluated solving saddle point equations under the assumption of replica symmetry, a method which, by taking into account only the term linear in  $N$  of the input information, is equivalent to assuming the noise to be large. Within this limitation, we analyze the dependence of the information on the ratio  $M/N$ , on the selectivity of the input units and on the level of the output noise. We show analytically, and confirm numerically, that in the limit of a linear transfer function and of a small ratio between output and input noise, the output information approaches asymptotically the information carried in input. Finally, we show that the information loss in output does not depend much on the structure of the stimulus, whether purely continuous, purely discrete or mixed, but only on the position of the threshold nonlinearity, and on the ratio between input and output noise.

## I. INTRODUCTION

Recent analyses of extracellular recordings performed in two motor areas of behaving monkeys have tried to clarify how information about movements is transmitted and received from higher to lower stages of processing, and to identify distinct roles of the two areas in the planning and execution of movements [1]. Although this study failed to produce clearcut results, it remains interesting to try and understand, from a more theoretical point of view, how information about multi-dimensional correlates of neural activity may be transmitted from the input to the output of a simple network. In fact, a theoretical study is still lacking, which explores how the coding of stimuli with continuous as well as discrete dimensions is transferred across a network.

Information theory [2] has been widely used in the theory of communication, in presence of both binary [3, 4, 5] and linear [6, 7] or weakly non-linear [8] channels. Moreover it has been recently proposed as an effective tool to explore the coding properties of neurons (see for example [9, 10, 11]), via both direct estimates from real data (for a review see [12]) and pure theoretical modelling [13, 14, 15, 16, 17, 18].

The *mutual information* provides a quantitative and flexible measure of the efficiency of single cells or of population of cells in coding external stimuli and events relevant to behaviour: high values of the mutual information are obtained when the correlates can be discriminated with a small uncertainty on the basis of the neural responses; moreover the same formalism can be adapted to explore different types of code, from simple time-averaged rates, to more sophisticated descriptions, where the exact temporal sequence of action potentials is considered to be relevant.

In a previous report [13] the mutual information between the time averaged rates of a finite population of  $N$  units and a set of correlates, which have both a discrete and a continuous angular dimension, has been evaluated analytically in the limit of large noise. This parameterization of the correlates can be applied to movements performed in a given direction and classified according to different "types"; yet it is equally applicable to other correlates, like visual stimuli characterized by an orientation and a discrete feature (colour, shape, etc..), or in general to any correlate which can be identified by an angle and a "type". In this study, we extend the analysis performed for one population, to consider two interconnected areas, and we evaluate the mutual information between the firing rates of a finite population of  $M$  output neurons and a set of continuous+discrete stimuli, given that the rate distribution in input is known. In input, a threshold nonlinearity has been shown to lower the information about the stimuli in a simple manner, which can be expressed as a renormalization of the noise [13]. How does the information in the output depend on the same nonlinearity? How does it depend on the noise in the output units? Is the information transmission from input to output sensitive to the structure of the correlate, whether discrete or continuous?

We address these issues by calculating the mutual information, using the replica trick and under the assumption of replica symmetry (see for example [19]).

Saddle point equations are solved numerically. We analyze how the information transmission depends on the parameters of the model, i.e. the level of output and input noise, on the ratio between the two population sizes, as well as on the tuning curve with respect to the continuous correlate, and on number of discrete correlates.

The input-output transfer function is a crucial element in the model. Many earlier theoretical and simulation studies [20] have mainly focused on binary and the sigmoidal functions; yet more recent investigations [21, 22] have shown that the current-to-frequency transduction typical of real neurons is well captured, away from saturation, by a threshold-linear function. Such a function combines the threshold of real neurons, the linear behaviour typical of pyramidal neurons above threshold, and the accessibility to a full analytical treatment [14, 23], as demonstrated here, too. For the sake of analytical feasibility, however, we take the input units to be purely gaussian. Therefore it should be kept in mind, in considering the final results, that the threshold nonlinearity is only applied to the output units.

## II. THE MODEL

In analogy to the model studied in [13] we consider a set of  $N$  input units which fire to an external continuous+discrete stimulus, parameterized by an angle  $\vartheta$  and a discrete variable  $s$ , with a gaussian distribution:

$$p(\{\eta_j\}|\vartheta, s) = \prod_{j=1}^N \frac{1}{\sqrt{2\pi\sigma^2}} \exp - \left[ (\eta_j - \tilde{\eta}_j(\vartheta, s))^2 / 2\sigma^2 \right]; \quad (1)$$

$\eta_j$  is the firing rate in one trial of the  $j^{th}$  input neuron, while the mean of the distribution,  $\tilde{\eta}_j(\vartheta, s)$  is written:

$$\tilde{\eta}_j(\vartheta, s) = \varepsilon_s^j \bar{\eta}_j(\vartheta) + (1 - \varepsilon_s^j) \eta^f; \quad (2)$$

$$\bar{\eta}_j(\vartheta - \vartheta_j^0) = \eta^0 \cos^{2m} \left( \frac{\vartheta - \vartheta_j^0}{2} \right); \quad (3)$$

where  $\varepsilon_s^j$  is a quenched random variable distributed between 0 and 1,  $\vartheta_i^0$  is the preferred direction for neuron  $i$ . According to eq.(2) neurons fire at an average firing rate which modulates with  $\vartheta$  with amplitude  $\varepsilon_s$ , or takes a fixed value  $\eta^f$ , independently of  $\vartheta$ , with amplitude  $1 - \varepsilon_s$ .

We assume that quenched disorder is uncorrelated and identically distributed across units and across the  $K$  discrete correlates, and that for each neuron all preferred directions are equally likely:

$$\varrho(\{\varepsilon_s^i\}) = \prod_{i,s} \varrho(\varepsilon_s^i) = [\varrho(\varepsilon)]^{NK} \quad (4)$$

$$\varrho(\{\vartheta_i^0\}) = [\varrho(\vartheta^0)]^N = \frac{1}{(2\pi)^N}.$$

In [13] it has been shown that a cosinusoidal shaped function as in eq.(2) is able to capture the main features of directional tuning of real neurons in motor cortex. Moreover it has been shown that the presence of negative firing rates in the distribution (1), which is not biologically plausible, does not alter information values, with respect to a more realistic choice for the firing distribution, in that it leads to the same curves except for a renormalization of the noise.

Output neurons are connected to input neurons via uncorrelated gaussian connection weights  $J_{ij}$ . Each output neuron performs a linear summation of the inputs; the outcome is distorted by a gaussian distributed fast noise  $\delta_i$  and then thresholded, as in the following:

$$\xi_i = [\xi_i^0 + \sum_j c_{ij} J_{ij} \eta_j + \delta_i]^+; \quad i = 1..M, j = 1..N \quad (5)$$

In eq.(5)  $\xi_i^0$  is a threshold term,  $c_{ij}$  is a (0,1) binary variable, with mean  $c$ , which expresses the sparsity or dilution of the connectivity matrix, and

$$\langle (J_{ij})^2 \rangle = \sigma_J^2; \quad \langle J_{ij} \rangle = 0; \quad (6)$$

$$\langle (\delta_i)^2 \rangle = \sigma_\delta^2; \quad \langle \delta_i \rangle = 0; \quad (7)$$

$$\begin{aligned} p(c_{ij}=1) &= c; \\ p(c_{ij}=0) &= 1 - c; \end{aligned} \quad (8)$$

$$[x]^+ = x\Theta(x). \quad (9)$$

### III. ANALYTICAL ESTIMATION OF THE MUTUAL INFORMATION

We aim at estimating the mutual information between the output patterns of activity and the continuous+discrete stimuli:

$$I(\{\xi_i\}, \vartheta \otimes s) = \left\langle \sum_{s=1}^K \int d\vartheta \int \prod_i d\xi_i p(\vartheta, s) p(\{\xi_i\}|\vartheta, s) \log_2 \frac{p(\{\xi_i\}|\vartheta, s)}{p(\{\xi_i\})} \right\rangle_{\varepsilon, \vartheta^0, c, J, \delta}; \quad (10)$$

$$p(\{\xi_i\}|\vartheta, s) = \int \prod_j d\eta_j p(\{\xi_i\}|\{\eta_j\}) p(\{\eta_j\}|\vartheta, s); \quad (11)$$

where the distribution  $p(\{\xi_i\}|\{\eta_j\})$  is determined by the threshold linear relationship (5),  $p(\{\eta_j\}|\vartheta, s)$  is given in eq.(1) and  $\langle \dots \rangle_{\varepsilon, \vartheta^0, c, J, \delta}$  is a short notation for the average across the quenched variables  $\{\varepsilon_s^i\}, \{\vartheta_i^0\}, \{J_{ij}\}, \{c_{ij}\}$  and on the fast noise  $\{\delta_i\}$ .

Contrary to the other quenched variables,  $\{\varepsilon_s^i\}, \{\vartheta_i^0\}, \{J_{ij}\}, \{c_{ij}\}$ , the variable  $\delta_i$  in eq.(5) is annealed: integration of relationships (5) across a zero mean gaussian distribution of  $\delta_i$  with variance  $\sigma_\delta^2$  yields a gaussian distribution in  $\xi_i$  with variance  $\sigma_\delta^2$ . We assume that the stimuli are equally likely:  $p(\vartheta, s) = 1/2\pi K$ .

Eq.(10) can be written as:

$$I(\{\xi_i\}, \vartheta \otimes s) = \langle H(\{\xi_i\}|\vartheta, s) \rangle_{\vartheta, s} - H(\{\xi_i\}) \quad (12)$$

with:

$$\langle H(\{\xi_i\}|\vartheta, s) \rangle_{\vartheta, s} = \left\langle \sum_s \int d\vartheta \int \prod_i d\xi_i p(\vartheta, s) p(\{\xi_i\}|\vartheta, s) \log_2 p(\{\xi_i\}|\vartheta, s) \right\rangle_{\varepsilon, \vartheta^0, c, J, \delta}; \quad (13)$$

$$\begin{aligned} H(\{\xi_i\}) &= \left\langle \sum_s \int d\vartheta \int \prod_i d\xi_i p(\vartheta, s) p(\{\xi_i\}|\vartheta, s) \right. \\ &\quad \left. \log_2 \left[ \sum_{s'} \int d\vartheta' p(s', \vartheta') p(\{\xi_i\}|\vartheta', s') \right] \right\rangle_{\varepsilon, \vartheta^0, c, J, \delta}. \end{aligned} \quad (14)$$

The analytical evaluation of  $\langle H(\{\xi_i\}|\vartheta, s) \rangle_{\vartheta, s}$  can be performed inserting eq.(11) in the expression (13), and using the replica trick [19] to get rid of the sums under logarithm; since these sums already multiply the logarithm, all replica indexes run from 1 up to  $n+1$ :

$$\begin{aligned} &\langle H(\{\xi_i\}|\vartheta, s) \rangle_{\vartheta, s} = \\ &\lim_{n \rightarrow 0} \frac{1}{n \ln 2} \left( \left\langle \sum_s \int d\vartheta p(\vartheta, s) \int \prod_{j, \alpha} d\eta_j^\alpha \prod_{j, \alpha} p(\eta_j^\alpha|\vartheta, s) \int \prod_i d\xi_i \prod_{j, \alpha} p(\xi_i|\{\eta_j^\alpha\}) \right\rangle_{\varepsilon, \vartheta^0, c, J, \delta} - 1 \right) \end{aligned} \quad (15)$$

To take into account the threshold-linear relation (5) we consider the following equalities:

$$\begin{aligned} \int d\xi_i \prod_{\alpha} p(\xi_i | \{\eta_j^{\alpha}\}) &= \prod_{\alpha} p(\xi_i = 0 | \{\eta_i^{\alpha}\}) + \int_0^{\infty} d\xi_i \prod_{\alpha} p(\xi_i | \{\eta_i^{\alpha}\}) = \\ \int_{-\infty}^0 \prod_{\alpha} d\xi_i^{\alpha} \delta(\xi_i^{\alpha} - \xi_i^0 - \sum_j c_{ij} J_{ij} \eta_j^{\alpha} - \delta_i^{\alpha}) &+ \int_0^{\infty} d\xi_i \prod_{\alpha} \delta(\xi_i - \xi_i^0 - \sum_j c_{ij} J_{ij} \eta_j^{\alpha} - \delta_i^{\alpha}). \end{aligned} \quad (16)$$

Inserting eq.(16) in eq.(15) one obtains:

$$\begin{aligned} \langle H(\{\xi_i\} | \vartheta, s) \rangle_{\vartheta, s} &= \lim_{n \rightarrow 0} \frac{1}{n \ln 2} \left( \sum_s \int d\vartheta p(\vartheta, s) \int \prod_{j, \alpha} d\eta_j^{\alpha} \left\langle \prod_{j, \alpha} p(\eta_j^{\alpha} | \vartheta, s) \right\rangle_{\varepsilon, \vartheta^0} \right. \\ &\prod_i \left[ \int_{-\infty}^0 \prod_{\alpha} d\xi_i^{\alpha} \left\langle \prod_{\alpha} \delta(\xi_i^{\alpha} - \xi_i^0 - \sum_j c_{ij} J_{ij} \eta_j^{\alpha} - \delta_i^{\alpha}) \right\rangle_{c, J, \delta} \right. \\ &\left. \left. + \int_0^{\infty} d\xi_i \left\langle \prod_{\alpha} \delta(\xi_i - \xi_i^0 - \sum_j c_{ij} J_{ij} \eta_j^{\alpha} - \delta_i^{\alpha}) \right\rangle_{c, J, \delta} \right] - 1 \right). \end{aligned} \quad (17)$$

The average across the quenched disorder  $c, J, \delta$  in eq.(17) can be performed in a very similar way as shown in [22]: using the integral representation for each  $\delta$  function, gaussian integration across  $J, \delta$  is standard; the average on  $\{c_{ij}\}$  can be performed assuming large the number  $N$  of input neurons, that is for very small  $c$ .

The final outcome for  $\langle H(\{\xi_i\} | \vartheta, s) \rangle_{\vartheta, s}$  reads:

$$\begin{aligned} \langle H(\{\xi_i\} | \vartheta, s) \rangle_{\vartheta, s} &= \lim_{n \rightarrow 0} \frac{1}{n \ln 2} \left( \sum_s \int d\vartheta p(\vartheta, s) \int \prod_{j, \alpha} d\eta_j^{\alpha} \left\langle \prod_{j, \alpha} p(\eta_j^{\alpha} | \vartheta, s) \right\rangle_{\varepsilon, \vartheta^0} \right. \\ &\left[ \int_{-\infty}^0 \prod_{\alpha} d\xi^{\alpha} \int \prod_{\alpha} \frac{dx^{\alpha}}{2\pi} e^{-(\sigma_{\delta}^2/2) \sum_{\alpha} (x^{\alpha})^2} e^{-(C\sigma_J^2/2N) \sum_{\alpha, \beta} x^{\alpha} x^{\beta} \sum_j \eta_j^{\alpha} \eta_j^{\beta}} e^{-i \sum_{\alpha} (\xi^{\alpha} - \xi_0) x^{\alpha}} \right. \\ &\left. \left. + \int_0^{\infty} d\xi \int \prod_{\alpha} \frac{dx^{\alpha}}{2\pi} e^{-(\sigma_{\delta}^2/2) \sum_{\alpha} (x^{\alpha})^2} e^{-(C\sigma_J^2/2N) \sum_{\alpha, \beta} x^{\alpha} x^{\beta} \sum_j \eta_j^{\alpha} \eta_j^{\beta}} e^{-i(\xi - \xi_0) \sum_{\alpha} x^{\alpha}} \right]^M - 1 \right) \end{aligned} \quad (18)$$



where we have put  $c \rightarrow C/N$ .

Integration on  $\{x^\alpha\}$  is straightforward. Integration on  $\{\eta_i^\alpha\}$  can be performed introducing  $(n+1)^2$  auxiliary variables  $z_{\alpha\beta} = \frac{1}{N} \sum_j \eta_j^\alpha \eta_j^\beta$  via  $\delta$  functions expressed in their integral representation. Considering the expression (1) for the input distribution and with some rearrangement of the terms the final result can be expressed as:

$$\begin{aligned} \langle H(\{\xi_i\}|\vartheta, s) \rangle_{\vartheta, s} = & \quad (19) \\ \lim_{n \rightarrow 0} \frac{1}{n \ln 2} \left( \int \prod_{\alpha, \beta} \frac{dz_{\alpha\beta}}{2\pi/N} \int \prod_{\alpha, \beta} d\tilde{z}_{\alpha\beta} e^{iN \sum_{\alpha, \beta} z_{\alpha\beta} \tilde{z}_{\alpha\beta}} e^{-\frac{N}{2} Tr \ln \Sigma} \sum_s \int d\vartheta p(\vartheta, s) \left\langle e^{-\sum_{\alpha, \beta} (\delta_{\alpha\beta} - \Sigma_{\alpha\beta}^{-1}) \tilde{\eta}(\vartheta, s)^2 / 2\sigma^2} \right\rangle_{\varepsilon, \vartheta^0}^N \right. \\ & \left. e^{-\frac{M}{2} Tr \ln G} \left[ \int_{-\infty}^0 \prod_{\alpha} \frac{d\xi^\alpha}{\sqrt{2\pi}} e^{-\sum_{\alpha, \beta} (\xi^\alpha - \xi_0)(G_{\alpha\beta}^{-1}/2)(\xi^\beta - \xi_0)} + \int_0^\infty \frac{d\xi}{(2\pi)^{\frac{n+1}{2}}} e^{-\sum_{\alpha, \beta} (G_{\alpha\beta}^{-1}/2)(\xi - \xi_0)^2} \right]^M - 1 \right), \end{aligned}$$

where:

$$\begin{aligned} \Sigma_{\alpha\beta} &= \delta_{\alpha\beta} + 2\sigma^2 i \tilde{z}_{\alpha\beta}; \\ G_{\alpha\beta} &= \sigma_\delta^2 \delta_{\alpha\beta} + C\sigma_J^2 z_{\alpha\beta}. \end{aligned} \quad (20)$$

The evaluation of  $H(\{\xi_i\})$ , eq.(14), can be carried out in a very similar way, introducing replicas in the continuous+discrete stimulus space. The final result reads:

$$\begin{aligned} H(\{\xi_i\}) &= \lim_{n \rightarrow 0} \frac{1}{n \ln 2} \left( \int \prod_{\alpha, \beta} \frac{dz_{\alpha\beta}}{2\pi/N} \int \prod_{\alpha, \beta} d\tilde{z}_{\alpha\beta} e^{iN \sum_{\alpha, \beta} z_{\alpha\beta} \tilde{z}_{\alpha\beta}} e^{-\frac{1}{2} Tr \ln \Sigma} \right. \\ & \quad \sum_{s_1 \dots s_{n+1}} \int d\vartheta_1 \dots d\vartheta_{n+1} [p(\vartheta, s)]^{n+1} \left\langle e^{-\sum_{\alpha, \beta} (\delta_{\alpha\beta} - \Sigma_{\alpha\beta}^{-1}) \tilde{\eta}(\vartheta_\alpha, s_\alpha) \tilde{\eta}(\vartheta_\beta, s_\beta) / 2\sigma^2} \right\rangle_{\varepsilon, \vartheta^0}^N \\ & \quad \left. e^{-\frac{M}{2} Tr \ln G} \left[ \int_{-\infty}^0 \prod_{\alpha} \frac{d\xi^\alpha}{\sqrt{2\pi}} e^{-\sum_{\alpha, \beta} (\xi^\alpha - \xi_0)(G_{\alpha\beta}^{-1}/2)(\xi^\beta - \xi_0)} + \int_0^\infty \frac{d\xi}{(2\pi)^{\frac{n+1}{2}}} e^{-\sum_{\alpha, \beta} (G_{\alpha\beta}^{-1}/2)(\xi - \xi_0)^2} \right]^M - 1 \right). \end{aligned} \quad (21)$$

#### IV. REPLICA SYMMETRIC SOLUTION

The integrals in eq.(19),(21) cannot be solved without resorting to an approximation. In analogy to what is used in [14, 22], we use a saddle-point approximation (which in general would be valid in the limit  $M, N \rightarrow \infty$ ) and we assume replica symmetry [19] in the parameters  $\{z_{\alpha\beta}\}$ ,  $\{\tilde{z}_{\alpha\beta}\}$ . This allows to explicitly invert and diagonalize the matrices  $G, \Sigma$ :

$$\begin{aligned} z_{\alpha\alpha} &= z_0(n); \quad z_{\alpha\neq\beta} = z_1(n); \\ i\tilde{z}_{\alpha\alpha} &= \tilde{z}_0(n); \quad i\tilde{z}_{\alpha\neq\beta} = -\tilde{z}_1(n); \end{aligned} \quad (22)$$

In [22] it has been shown that the replica symmetric solution for the information transmitted by a threshold-linear net is stable in most of the phase diagram. A detailed study of the stability of the RS solution in the specific case of mixed continuous and discrete stimuli will be presented elsewhere [24]. The saddle point approximation seems to have more subtle implications in the present situation, as it will be discussed in the next section and in the final discussion.

In replica symmetry the mutual information can be expressed as follows:

$$\begin{aligned} I(\{\xi_i\}, \vartheta \otimes s) &= \lim_{n \rightarrow 0} \frac{1}{n \ln 2} \left\{ e^{N[(n+1)z_0^A \tilde{z}_0^A - n(n+1)z_1^A \tilde{z}_1^A - \frac{r}{2}(Tr \ln G(z_0^A, z_1^A) + F(z_0^A, z_1^A)) - \frac{1}{2}Tr \ln \Sigma(\tilde{z}_0^A, \tilde{z}_1^A) - H^A(\tilde{z}_0^A, \tilde{z}_1^A)]} \right. \\ &\quad \left. - e^{N[(n+1)z_0^B \tilde{z}_0^B - n(n+1)z_1^B \tilde{z}_1^B - \frac{r}{2}(Tr \ln G(z_0^B, z_1^B) + F(z_0^B, z_1^B)) - \frac{1}{2}Tr \ln \Sigma(\tilde{z}_0^B, \tilde{z}_1^B) - H^B(\tilde{z}_0^B, \tilde{z}_1^B)]} \right\}, \quad (23) \end{aligned}$$

with

$$F(z_0, z_1) = -2 \ln \left[ \int_{-\infty}^0 \prod_{\alpha} \frac{d\xi^{\alpha}}{\sqrt{2\pi}} e^{-\sum_{\alpha,\beta} (\xi^{\alpha} - \xi_0)(G_{\alpha\beta}^{-1}/2)(\xi^{\beta} - \xi_0)} + \int_0^{\infty} \frac{d\xi}{(2\pi)^{\frac{n+1}{2}}} e^{-\sum_{\alpha,\beta} (G_{\alpha\beta}^{-1}/2)(\xi - \xi_0)^2} \right]; \quad (24)$$

$$H^A(\tilde{z}_0, \tilde{z}_1) = -\frac{1}{N} \ln \left[ \sum_s \int d\vartheta p(\vartheta, s) \left\langle e^{-\sum_{\alpha,\beta} (\delta_{\alpha\beta} - \Sigma_{\alpha\beta}^{-1}) \tilde{\eta}(\vartheta, s)^2 / 2\sigma^2} \right\rangle_{\varepsilon, \vartheta^0}^N \right]; \quad (25)$$

$$H^B(\tilde{z}_0, \tilde{z}_1) = -\frac{1}{N} \ln \left[ \sum_{s_1 \dots s_{n+1}} \int d\vartheta_1 \dots d\vartheta_{n+1} [p(\vartheta, s)]^{n+1} \left\langle e^{-\sum_{\alpha,\beta} (\delta_{\alpha\beta} - \Sigma_{\alpha\beta}^{-1}) \tilde{\eta}(\vartheta_{\alpha}, s_{\alpha}) \tilde{\eta}(\vartheta_{\beta}, s_{\beta}) / 2\sigma^2} \right\rangle_{\varepsilon, \vartheta^0}^N \right]. \quad (26)$$

We have set  $r = \frac{M}{N}$  and  $z_0^{A,B}, \tilde{z}_0^{A,B}, z_1^{A,B}, \tilde{z}_1^{A,B}$  are the solutions of the saddle point equations:

$$\begin{aligned} z_0^{A,B} &= \frac{\partial}{\partial \tilde{z}_0} \left[ \frac{1}{2} Tr \ln \Sigma(\tilde{z}_0, \tilde{z}_1) + H^{A,B}(\tilde{z}_0, \tilde{z}_1) \right]; \\ z_1^{A,B} &= -\frac{1}{n} \frac{\partial}{\partial \tilde{z}_1} \left[ \frac{1}{2} Tr \ln \Sigma(\tilde{z}_0, \tilde{z}_1) + H^{A,B}(\tilde{z}_0, \tilde{z}_1) \right]; \\ \tilde{z}_0^{A,B} &= \frac{\partial}{\partial z_0} \frac{r}{2} [Tr \ln G(z_0, z_1) + F(z_0, z_1)]; \\ \tilde{z}_1^{A,B} &= -\frac{1}{n} \frac{\partial}{\partial z_1} \frac{r}{2} [Tr \ln G(z_0, z_1) + F(z_0, z_1)]. \end{aligned} \quad (27)$$

All the equations must be evaluated in the limit  $n \rightarrow 0$ . It is easy to check that all terms in the exponent in eq.(23) are order  $n$ . In fact, since when  $n \rightarrow 0$  only one replica remains, one has:

$$\begin{aligned} \lim_{n \rightarrow 0} Tr \ln G(z_0, z_1) + F(z_0, z_1) &= 0 \rightarrow \\ Tr \ln G(z_0, z_1) + F(z_0, z_1) &\simeq n \frac{\partial}{\partial n} [Tr \ln G(z_0, z_1) + F(z_0, z_1)]_{|n=0}. \end{aligned} \quad (28)$$

Therefore, from the saddle point equations,  $\tilde{z}_0^{A,B}$  are order  $n$  and  $Tr \ln \Sigma$  is also order  $n$ :

$$Tr \ln \Sigma \simeq n \frac{\partial}{\partial n} Tr \ln \Sigma|_{n=0}. \quad (29)$$

Since  $\tilde{z}_0^{A,B} = n \tilde{z}_0^{A,B}$ , it is easy to check by explicit evaluation that, when  $n \rightarrow 0$ , all the  $n+1$  diagonal terms among the matrix elements  $\{\delta_{\alpha\beta} - \Sigma_{\alpha\beta}^{-1}\}$  are order  $n$  and all the  $n(n+1)$  out-of-diagonal terms are order 1. Then all terms in the exponent of eqs.(25),(26) are order  $n$ , and we can expand the exponentials, which allows us to perform the quenched averages across  $\{\varepsilon, \vartheta^0\}$ . Considering the expression of  $\tilde{\eta}(\vartheta, s)$ , eq.(2), one obtains:

$$\begin{aligned} H^A(\tilde{z}_0^A, \tilde{z}_1^A) &\simeq n(\tilde{z}_0^A - \tilde{z}_1^A)\Lambda_\eta^1; \\ H^B(\tilde{z}_0^B, \tilde{z}_1^B) &\simeq n \left( (\tilde{z}_0^B - \tilde{z}_1^B)\Lambda_\eta^1 + \frac{\tilde{z}_1^B}{1 + 2\sigma^2\tilde{z}_1^B} [\Lambda_\eta^1 - \Lambda_\eta^2] \right); \end{aligned} \quad (30)$$

$$\begin{aligned} \Lambda_\eta^1 &= \sum_s \int d\vartheta p(s, \vartheta) \langle [\tilde{\eta}(\vartheta, s)]^2 \rangle_{\varepsilon, \vartheta^0} \\ &= (\eta^0)^2 \left[ (A_2 + \alpha^2 - 2\alpha A_1) \langle \varepsilon^2 \rangle_\varepsilon + \alpha^2 + 2\alpha(A_1 - \alpha) \langle \varepsilon \rangle_\varepsilon \right]; \end{aligned} \quad (31)$$

$$\begin{aligned} \Lambda_\eta^2 &= \sum_{s_1, s_2} \int d\vartheta_1 d\vartheta_2 [p(s, \vartheta)]^2 \langle \tilde{\eta}(\vartheta_1, s_1) \tilde{\eta}(\vartheta_2, s_2) \rangle_{\varepsilon, \vartheta^0} \\ &= (\eta^0)^2 \left[ (A_1 - \alpha)^2 \left( \frac{K-1}{K} \langle \varepsilon \rangle_\varepsilon^2 + \frac{1}{K} \langle \varepsilon^2 \rangle_\varepsilon \right) + \alpha^2 + 2\alpha(A_1 - \alpha) \langle \varepsilon \rangle_\varepsilon \right]; \end{aligned} \quad (32)$$

$$A_1 = \frac{1}{2^{2m}} \binom{2m}{m}; \quad A_2 = \frac{1}{2^{4m}} \binom{4m}{2m}; \quad \alpha = \frac{\eta^f}{\eta^0}. \quad (33)$$

A similar expansion in  $n$  for  $Tr \ln \Sigma(\tilde{z}_0, \tilde{z}_1)$  and for  $Tr \ln G(z_0, z_1) + F(z_0, z_1)$  allows to derive explicitly the saddle point equations:

$$\begin{aligned}
z_0^{A,B} &= \sigma^2 + \Lambda_\eta^1; \\
z_1^A &= \frac{2\sigma^4 \tilde{z}_1^A}{2\sigma^2 \tilde{z}_1^A + 1} + \Lambda_\eta^1; \\
z_1^B &= \frac{2\sigma^4 \tilde{z}_1^B}{2\sigma^2 \tilde{z}_1^B + 1} + \left[ 1 - \frac{1}{(1 + 2\sigma^2 \tilde{z}_1^B)^2} \right] \Lambda_\eta^1 + \frac{1}{(1 + 2\sigma^2 \tilde{z}_1^B)^2} \Lambda_\eta^2; \\
\tilde{z}_1^{A,B} &= -C\sigma_J^2 \frac{r}{2} \left\{ \sigma \left( \frac{\xi^0}{\sqrt{p+q}} \right) \frac{\xi^0}{(p+q)^{\frac{3}{2}}} - \frac{1}{p} \text{erf} \left( \frac{\xi^0}{\sqrt{p+q}} \right) \right. \\
&\quad \left. + \int_{-\infty}^{\infty} Dt \left[ 1 + \ln \left( \text{erf} \left( -\frac{\xi^0 - t\sqrt{q}}{\sqrt{p}} \right) \right) \right] \sigma \left( \frac{\xi^0 - t\sqrt{q}}{\sqrt{p}} \right) \frac{1}{p^{\frac{3}{2}}} \left[ \xi^0 - t \frac{q+p}{\sqrt{q}} \right] \right\};
\end{aligned} \tag{34}$$

where:

$$\text{erf}(x) = \int_{-\infty}^x Dx' = \int_{-\infty}^x dx' \sigma(x'); \quad \sigma(x) = \frac{1}{\sqrt{2\pi}} e^{-\frac{x^2}{2}};$$

$$p = \sigma_\delta^2 + C\sigma_J^2(z_0 - z_1); \quad q = C\sigma_J^2 z_1.$$

From the expression of  $z_0^{A,B}$  in eq.(34), it is easy to verify that the dependence on  $\tilde{z}_0^{A,B}$  in eq.(30), which might affect the information in eq.(23), cancels out with the products  $z_0^A \tilde{z}_0^A, z_0^B \tilde{z}_0^B$  which should contribute to the information in the limit  $n \rightarrow 0$  (see eq.(23)). Therefore, since  $z_0^{A,B}$  is known and  $z_1^{A,B}$  depends only on  $\tilde{z}_1^{A,B}$ , the mutual information can be expressed as a function of  $z_1^{A,B}, \tilde{z}_1^{A,B}$ , which in turn are to be determined self-consistently by the saddle point equations.

The average information per input cell can be written, finally:

$$\frac{I}{N}(\{\xi_i\}, \vartheta \otimes s) = \frac{1}{\ln 2} \left\{ \tilde{z}_1^B z_1^B - \tilde{z}_1^A z_1^A + r \left[ \Gamma_1(z_0^B, z_1^B) - \Gamma_1(z_0^A, z_1^A) \right] + \Gamma_2^B(\tilde{z}_1^B) - \Gamma_2^A(\tilde{z}_1^A) \right\}, \quad (35)$$

with

$$\begin{aligned} \Gamma_1(z_0, z_1) = & -\sigma \left( \frac{\xi^0}{\sqrt{p+q}} \right) \frac{\xi^0 p}{2(p+q)^{\frac{3}{2}}} + \frac{1}{2} \ln p \operatorname{erf} \left( \frac{\xi^0}{\sqrt{p+q}} \right) \\ & - \int_{-\infty}^{\infty} Dt \operatorname{erf} \left( -\frac{\xi^0 - t\sqrt{q}}{\sqrt{p}} \right) \ln \left[ \operatorname{erf} \left( -\frac{\xi^0 - t\sqrt{q}}{\sqrt{p}} \right) \right]; \end{aligned} \quad (36)$$

$$\Gamma_2^A(\tilde{z}_1^A) = +\frac{1}{2} \ln(1 + 2\sigma^2 \tilde{z}_1^A) - \tilde{z}_1^A(\sigma^2 + \Lambda_\eta^1); \quad (37)$$

$$\Gamma_2^B(\tilde{z}_1^B) = \frac{1}{2} \ln(1 + 2\sigma^2 \tilde{z}_1^B) - \tilde{z}_1^B(\sigma^2 + \Lambda_\eta^1) + \frac{\tilde{z}_1^B}{1 + 2\sigma^2 \tilde{z}_1^B} [\Lambda_\eta^1 - \Lambda_\eta^2]. \quad (38)$$

The expression for the mutual information only contains terms linear in either  $N$  or  $M$ . Since the last of the saddle-point equations, (34), contains  $r$ , if one fixes  $N$  and increases  $M$  the information grows non-linearly, because the position of the saddle point varies. It turns out that, as shown below, the growth is only very weakly sublinear, at least when  $M \leq N$ . Analogously, fixing  $M$  and varying  $N$  we would find a non-linearity due to the  $r$ -dependence of the saddle point. If  $r$  is fixed and  $N$  and  $M$  grow together, the information rises purely linearly.

What our analytical treatment misses out, however, is the nonlinearity required to appear as the mutual information approaches its ceiling, the entropy of the stimulus set. The approach to this saturating value was described at the input stage [15, 16], where also the

initial linear rise (in  $N$ ) was obtained in the large noise limit [13, 15]. Our saddle point method is in same sense similar to taking a large (input) noise limit,  $\sigma \rightarrow \infty$ , to its leading (order  $N/\sigma^2$ ) term. It is possible that the saddle point method could be extended, to account also for successive terms in a large noise expansion. This would probably require integrating out the fluctuations around the saddle point, but by carefully analysing the relation of different replicas to different values of the quenched variables. We leave this possible extension to future work. The present calculation, therefore, although employing a saddle point method which is usually applicable for large  $N$  and  $M$ , should be considered effectively as yielding the initial linear rise in the mutual information, the one observed with  $M$  small.

## V. NUMERICAL RESULTS

Eq.(34) for  $\tilde{z}_1^{A,B}$  has been solved numerically using a Matlab Code. Convergence to self-consistency has been found already after 50 iterations with an error lower than  $10^{-10}$ .

Fig.1 shows the mutual information as a function of the output population size, for an input population size equal to 100 cells. This is contrasted with the information in the input units, about exactly the same set of correlates, calculated as in [13], by keeping only the leading (linear) term in  $N$ . In fact, in [13] the mutual information carried by a finite population of neurons firing according to eq.(1) had been evaluated analytically, in the limit of large noise, by means of an expansion in  $N(\eta^0)^2/4\sigma^2$ . To linear order in  $N$  the analytical

expression for the information carried by  $N$  input neurons reads:

$$I_{input}(\{\eta_j\}, \vartheta \otimes s) = \frac{1}{\ln 2} \frac{N}{2\sigma^2} (\Lambda_\eta^1 - \Lambda_\eta^2); \quad (39)$$

where  $\Lambda_\eta^1, \Lambda_\eta^2$  are defined, again, as in eqs.(31), (32). In analogy to what had been done in [14] we have set  $C\sigma_J^2 = 1$ . As evident from the graph, also the output information is essentially linear up to a value of  $r \simeq 0.5$ , and quasi-linear even for  $r = 1$ . It should be reminded, again, that our saddle point method only takes into account the term linear in  $N$  in the information *input* units carry about the stimulus. It is not possible, therefore, for eq.(35) to reproduce the saturation in the mutual information as it approaches the entropy of the stimulus set (which is finite, if one considers only discrete stimuli). The nearly linear behaviour in  $M$  thus reflects the linear behaviour in  $N$  induced, in the intermediate quantity (the information available at the input stage), by our saddle point approximate evaluation.

As it is clear from the comparison in Fig.1, when the two populations of units are affected by the same noise the input information is considerably higher than the output one. This is expected, since output and input noise sum up while influencing the firing of output neurons, but also because the input distribution is taken to be a pure gaussian, while the output rates are affected by a threshold. If the input-output tranformation were linear and the output noise much smaller than the input one, one would expect that output and input units would carry the same amount of information.



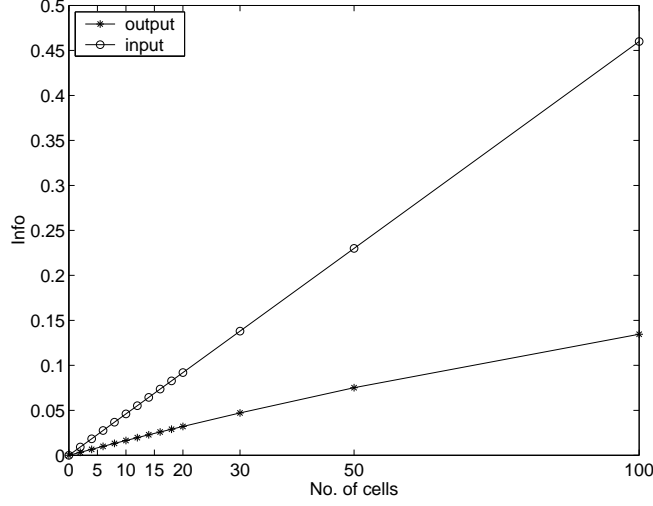


FIG. 1: Information rise, from eq.(35), as a function of the number  $M$  of output neurons.  $N = 100$ ;  $K = 4$ ;  $(\eta^0)^2 = 0.1$ ;  $\alpha = 0.2$ ;  $\xi^0 = -0.4$ ;  $\sigma^2 = 1$ ;  $m = 1$ ;  $C\sigma_J^2 = 1$ ;  $\sigma_\delta^2 = 1$ . The distribution  $\varrho(\varepsilon)$  in eq.(4) is just equal to  $1/3$  for each of the 3 allowed  $\varepsilon$  values of 0,  $1/2$  and 1. The upper curve is the linear term in the input information, calculated as a function of  $N$  as in [13] with identical parameters.

Briefly, in a linear network with zero output noise one has:

$$p(\{\xi_i\}|\{\eta_j\}) = \prod_i \delta(\xi_i - \sum_j c_{ij} J_{ij} \eta_j); \quad (40)$$

Considering eqs.(11),(1), an *effective* expression for the distribution  $p(\{\xi_i\}|\vartheta, s)$  can be obtained by direct integration of the  $\delta$  functions  $\delta(\xi_i - \sum_j c_{ij} J_{ij} \eta_j)$  via their integral representation, on  $\{\eta_j\}$ :

$$p(\{\xi_i\}|\vartheta, s) = \frac{1}{\sqrt{(2\pi)^M \det \Sigma}} e^{-\sum_{i,j} (\xi_i - \tilde{\xi}_i(\vartheta, s)) (\Sigma_{ij}^{-1}) / 2 (\xi_j - \tilde{\xi}_j(\vartheta, s))}; \quad (41)$$

$$\tilde{\xi}_i(\vartheta, s) = \sum_j c_{ij} J_{ij} \tilde{\eta}_j(\vartheta, s); \quad (42)$$

$$\Sigma_{ij} = \sigma^2 \sum_k c_{ik} J_{ik} c_{kj}^T J_{kj}^T; \quad (43)$$

This distribution is then used to evaluate both the equivocation, eq.(13), and the entropy of the responses, eq.(14). We do not report the calculation, that is straightforward and analogous to the one reported in [13]. The final result, which is valid for a finite population size  $M$ , and up to the linear approximation in  $M(\eta^0)^2/4\sigma^2$ , is analogous to eq.(39):

$$I_{lin}(\{\xi_i\}, \vartheta \otimes s) = \frac{1}{\ln 2} \frac{M}{2\sigma^2} (\Lambda_\eta^1 - \Lambda_\eta^2); \quad (44)$$

Thus, we expect that taking the limits  $\xi^0 \rightarrow \infty$  and  $r \rightarrow 0$  simultaneously in eq.(35), we should get to the same result: the output information should equal the input one when  $\sigma^2$  grows large.

From eq.(35) it is easy to show that:

$$\lim_{r \rightarrow 0} \lim_{\xi^0 \rightarrow \infty} I(\{\xi_i\}, \vartheta \otimes s) = \frac{1}{\ln 2} \frac{M}{2} \ln \left[ 1 + \frac{2C\sigma_J^2 (\Lambda_\eta^1 - \Lambda_\eta^2)}{\sigma_\delta^2 + 2C\sigma_J^2\sigma^2} \right]; \quad (45)$$

When  $\sigma^2 \gg \sigma_\delta^2, \Lambda_\eta^1, \Lambda_\eta^2$  one obtains exactly the linear limit, eq.(44). We have verified this analytical limit by studying numerically the approach to the asymptotic value of the mutual information. Fig.2 shows the dependence of output information on the output noise  $\sigma_\delta^2$ , for 4 different choices of the (reciprocal of the) threshold,  $\xi^0$ . A large value,  $\xi^0 = 10$ , implies linear output units. As expected, the output information, which always grows for decreasing values of the output noise, for  $\xi^0 = 10$  approaches asymptotically the input information. For increasing values of the output noise, the information vanishes with a typical sigmoid curve,

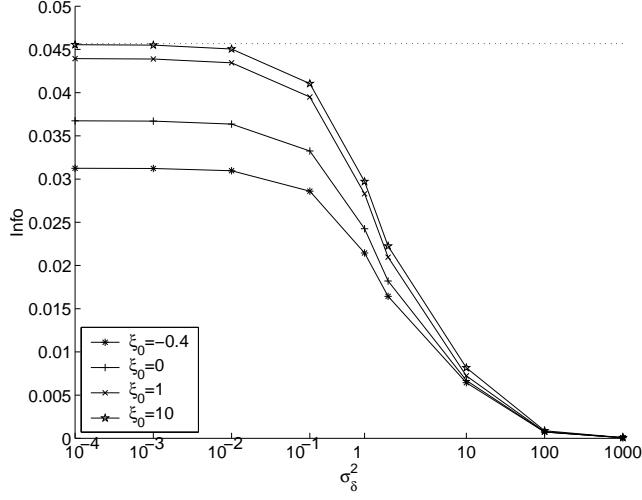


FIG. 2: Output information, from eq.(35), as a function of the output noise  $\sigma_\delta^2$ , for 4 different values of the output (reciprocal) threshold  $\xi^0$ . Logarithmic scale.  $N = 100$ ;  $K = 4$ ;  $M = 10$ ;  $(\eta^0)^2 = 0.1$ ;  $\alpha = 0.2$ ;  $\sigma^2 = 1$ ;  $m=1$ ;  $C\sigma_J^2 = 1$ . The distribution  $\varrho(\varepsilon)$  in eq.(4) is just equal to  $1/3$  for each of the 3 allowed  $\varepsilon$  values of 0,  $1/2$  and 1. The dotted line represents the asymptotic value of the input information, eq.(39), for  $N = 10$ .

with its point of inflection when the output matches the input noise.

We have then examined how the information in output (compared to the input) depends on the number  $K$  of discrete correlates and on the width of the tuning function (3), parametrized by  $m$ , with respect to the continuous correlate. Fig.3 shows a comparison between input and output information for a sample of 10 cells, as a function of  $K$ . Both curves quickly reach an asymptotic value, obtained by setting  $K \rightarrow \infty$  in eq.(32) for  $\Lambda_\eta^2$ . The relative information loss in output is roughly constant with  $K$ . A comparison is shown with the case where correlates are purely discrete, which is obtained by setting  $m = 0$  in eq.(3). The curves exhibit a similar behaviour, even if the rise with  $K$  is steeper, and the asymptotic values are higher. This may be surprising, but it is in fact a consequence of the specific model we have considered, eq.(2), where a unit has the same tuning curve to each

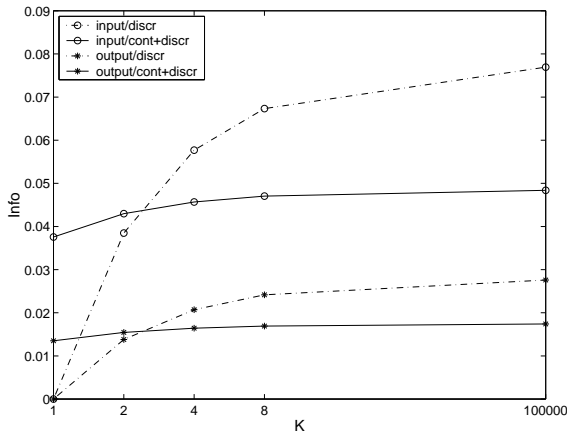


FIG. 3: Comparison between input and output information as a function of the number  $K$  of discrete correlates, for the case of continuous+discrete correlates ( $m = 1$ ) or with purely discrete correlates (obtained by setting  $m = 0$ ). In eq.(35) we have set  $N = 100$ ;  $r = 0.1$ ;  $\xi^0 = -0.4$ ;  $(\eta^0)^2 = 0.1$ ;  $\alpha = 0.2$ ;  $\sigma^2 = 1$ ;  $C\sigma_J^2 = 1$ ;  $\sigma_\delta^2 = 1$ . The distribution  $\varrho(\varepsilon)$  in eq.(4) is just equal to  $1/3$  for each of the 3 allowed  $\varepsilon$  values of 0,  $1/2$  and 1.

of the discrete correlates, only varying its amplitude with respect to a value constant in the angle. As  $K \rightarrow \infty$ , most of the mutual information is about the discrete correlates, and the tuning to the continuous dimension, present for  $m = 1$ , effectively adds noise to the discrimination among discrete cases, noise which is not present for  $m = 0$ .

With respect to the continuous dimension, the selectivity of the input units can be increased by varying the power  $m$  of the cosine from 0 (no selectivity) through 1 (very distributed encoding, as for the discrete correlates) to higher values (progressively narrower tuning functions). Fig.4 reports the resulting behaviour of the information in input and in output, for the case  $K = 1$  (only a continuous correlate) and  $K = 4$  (continuous+discrete correlates). Increasing selectivity implies a "sparser" [21] representation of the angle, the continuous variable, and hence less information, on average. However if the correlate is purely continuous there is an initial increase, before reaching the optimal sparseness. It

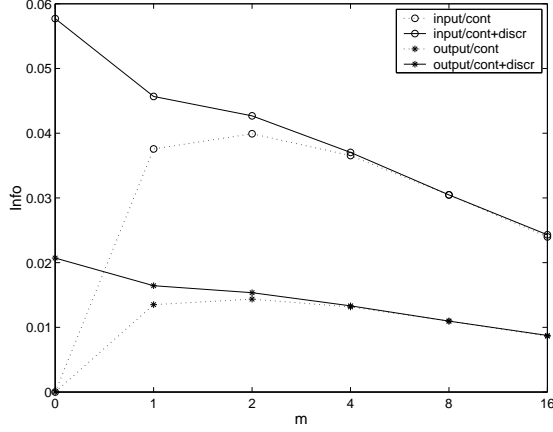


FIG. 4: Comparison between input and output information as a function of the selectivity along the continuous dimension, which is made sharper by increasing  $m$ .  $K = 1$  implies a purely continuous correlate, while the continuous+discrete case is obtained by setting  $K = 4$ . In eq.(35) we have set  $N = 100$ ;  $r = 0.1$ ;  $\xi^0 = -0.4$ ;  $(\eta^0)^2 = 0.1$ ;  $\alpha = 0.2$ ;  $m = 1$ ;  $C\sigma_J^2 = 1$ ;  $\sigma_\delta^2 = \sigma^2 = 1$ , in both cases. The distribution  $\varrho(\varepsilon)$  in eq.(4) is just equal to  $1/3$  for each of the 3 allowed  $\varepsilon$  values of 0,  $1/2$  and 1.

should be kept in mind, again, that the asymptotic equality of the  $K = 1$  and  $K = 4$  cases is a consequence of the specific model, eq.(2), which assigns the same preferred angle to each discrete correlate. The resolution with which the continuous dimension can be discriminated does not, within this model, improve with larger  $K$ , while the added contribution, of being able to discriminate among discrete correlates, decreases in relative importance as the tuning becomes sharper.

Figures 3 and 4 show that, as long as the output noise is non zero and the threshold is finite, information is lost going from input to output, but the information loss does not appear to depend on the structure and on the dimensionality of the correlate.

Note that, while the purely continuous case has been easily obtained by setting  $K = 1$  in the expression of  $\Lambda_\eta^2$ , eq.(32), for the purely discrete case it is enough to set  $m = 0$ .

## VI. SIMULATION RESULTS: INFORMATION ESTIMATES VIA DECODING

One way to test the range of validity of our analytical approximation is via numerical estimates of the information. In our specific case where we deal with populations of continuous neurons and with 4 different sources of quenched disorder, direct numerical integration is prohibitive. A more feasible method is to generate simulated data both in input and in output and then to estimate the information from the data, resorting to some algorithm.

Many previous studies (revised in [9]) have shown that information estimates from data are extremely sensitive to sampling and the distortion is the more serious the larger is the space of the possible configurations which has to be sampled. In our case where neurons are characterized by their time averaged continuous firing rates, a simple binning of the responses into discrete distributions results in a considerable distortion, which becomes even more serious since a sparse sampling is required to perform the average across the four quenched distributions.

Several procedures have been proposed to correct the bias affecting information estimates; some of them (see [9]) are based on regularizations like binning or smoothing; other ones rely on more theoretical approaches aiming at providing an analytical expression for the correction [25].

When the responses vary in a continuum and the population size is very large it has been suggested that the best estimate is obtained via *decoding*: the method consists in generating a *predicted* stimulus  $s'(\mathbf{r}_k)$  from each simulated response vector  $\mathbf{r}_k(s)$  in each trial  $k$  by matching  $\mathbf{r}_k(s)$  to the average response vector  $\mathbf{r}_{av}(s')$ , for all stimuli. The predicted stimulus will be the one corresponding to the best match. Summing on all the trials one can

derive a probability table  $p(s, s')$ ; then, the mutual information between the true and the pseudo-stimuli is computed instead of the original one, between stimuli and responses:

$$I(s, s') = \sum_{s=1}^p \sum_{s'=1}^p P(s, s') \log_2 \frac{P(s, s')}{P(s)P(s')}. \quad (46)$$

From a theoretical point of view the optimal transformation to derive the probability  $p(s'|\mathbf{r})$  is defined by Bayes rule (Bayesian decoding):

$$p(\mathbf{r}|s)p(s) = p(\mathbf{r})p(s|\mathbf{r}); \quad (47)$$

In our specific case the input distribution is defined in eq.(1), so that relationship (47) can be explicitly inverted; on the contrary the output distribution is not explicitly known and one has to fit some function to the responses to be able to invert the relationship (47). Further details about these procedures can be found in [9, 26].

Fig.5 shows the results of simulations for a sample of 20 output cells receiving from 1000 input cells. A MATLAB code has been used to generate data in an amount of 2000 responses per neuron per stimulus, where we have considered the simpler case of 4 purely discrete stimuli ( $m = 0$  in eq.3). The decoding in output has been optimized choosing a high value for the threshold  $\xi^0$ , so that the single cell output distribution, as derived from the simulated data, could be roughly fitted by a gaussian. For each population size we have chosen many random subsamples of units out of the whole population, both in input and in output, and we have then averaged the information value across subsamples. Quenched averages have been performed resorting to a sparse sampling.

The plot shows that the curves obtained via simulations (dashed lines) match the analytical prediction (solid lines) for a very small number of cells, but they deviate when the number of cells increases; since both the input and the output noise are large and the information values are much lower than the upper bound of 2 bits, this mismatch cannot be due to a deviation from linearity close to the ceiling regime. It is more probably an effect due to the distortion caused by the decoding, which is known to increase with the population size. The discrepancy between the true and the decoded information has also been recently investigated and quantified analytically [27].

The analytical approximation seems to have a wider applicability in output, where even for a population size larger than 4-5 cells the analytical curve falls within the error. This is mainly an effect due to the larger error characterizing the output information, which in turn is due to the stronger fluctuations in the information values across the different subsamples of cells. We have checked that the analytical results are always confirmed for a population size of 1 or 2 cells varying the number of discrete correlates and the value of the input and output noise.

We certainly cannot conclude from this that our analytical approximation is not valid for population sizes larger than 2-3 cells. On the contrary we are currently devising new algorithms to reduce the bias in the information estimates and preliminary results seem to suggest a much wider range of validity of the analytical approximation. A more detailed study comparing decoding to other algorithms will be published elsewhere [28].



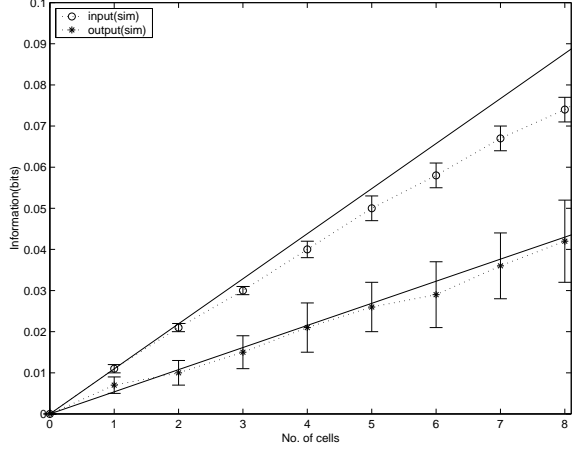


FIG. 5: Comparison between the analytical approximation (solid lines) and simulations (dashed lines) for the input and the output information.  $N = 1000$ ;  $K = 4$ ;  $r = 0.02$ ;  $\xi^0 = 2$ ;  $(\eta^0)^2 = 0.1$ ;  $\alpha = 0.1$ ;  $m = 0$ ;  $C\sigma_J^2 = 1$ ;  $\sigma_\delta^2 = \sigma^2 = 1$ . The distribution  $\varrho(\varepsilon)$  in eq.(4) is just equal to  $1/2$  for each of the 2 allowed  $\varepsilon$  values of 0 and 1

## VII. DISCUSSION

We have attempted to clarify how information about multi-dimensional stimuli, with both a continuous and a discrete dimension, is transmitted from a population of units with a known coding scheme, down to the next stage of processing.

Previous studies had focused on the mutual information between input and output units in a two-layer threshold-linear network either with learning [14] or with simple random connection weights [22].

More recent investigations have tried to quantify the efficiency of a population of units in coding a set of discrete [15] or continuous [16] correlates. The analysis in [15] has been then generalized to the more realistic case of multi-dimensional continuous+discrete correlates [13].

This work correlates with both research streams, in an effort to define a unique conceptual

framework for population coding. The main difference with the second group of studies is obviously the presence of the network linking input to output units. The main difference with the first two papers, instead, is the analysis of a distinct mutual information quantity: not between input and output units, but between correlates ("stimuli") and output units. In [15] it had been argued, for a number  $K$  of purely discrete correlates, that the information *about* the stimuli reduces to the information about the "reference" neural activity when  $K \rightarrow \infty$ . The reference activity is simply the mean response to a given stimulus when the information is measured from the variable, noisy responses around that means; or it can be taken to be the stored pattern of activity, when the retrieval of such patterns is considered, as in [14]. True, the information about the stimuli saturates at the entropy of the stimulus set, but for  $K \rightarrow \infty$  this entropy diverges, only the linear term in  $N$  is relevant [15], and the two quantities, information about the stimuli and information about the reference activity, coincide.

Our present saddle point calculation is only able to capture, effectively, the mutual information which is linear in the number of input units, as mentioned above. It fails to describe the approach to the saturating value, the entropy of the set of correlates, be this finite or infinite. Therefore, ours is close to a calculation of the information about a reference activity - in our case, the activity of the input units. The remaining difference is that we can take into account, albeit solely in the linear term, the dependence on  $K$  (through the equation for  $\Lambda_\eta^2$ , eq.(32)), without having to take the further limit  $K \rightarrow \infty$ .

Due to the presence of a threshold and of a non zero output noise the information in output is lower than that in input, and we have shown analytically that in the limit of a

noiseless, linear input-output transfer function the output information tends asymptotically to the input one. We have not, however, introduced a threshold in the input units, which would be necessary for a fair comparison. In an independent line of research, recent work [8] has also quantified the contribution to the mutual information, in a different model, of cubic and higher order non-linearities in the transfer function, by means of a diagrammatic expansion in a noise parameter. In [13] it has been shown that the effect of a threshold in the input units on the input information results merely in a renormalization of the noise. The resulting effect on the output information remains to be explored, possibly with similar methods.

Considering mixed continuous and discrete dimensions in our stimulus set, we had been wondering whether the information loss in output depended on the presence or absence of discrete or continuous dimensions in the stimulus structure. We have shown that for a fixed, finite level of noise this loss does not depend significantly on the structure of the stimulus, but solely on the relative magnitude of input and output noise, and on the position of the output threshold.

Our analytical efforts have been also motivated by the difficulty to perform a simulation study for this specific scheme of continuous rate coding in presence of several distinct sources of quenched disorder. Nonetheless we have performed some simulations using a *decoding* procedure to estimate the information from simulated data both in input and in output. Our results confirm previous findings in that the distortion due to decoding grows with the population size, so that the simulations confirm the analytical prediction only for a very small number of cells. We are currently devising new computational methods to improve the match

between the analytical and the simulation results.

Further developments of this analysis include the evaluation of the output information in presence of learning, in line with [14], and with correlations in the firing of input units.

A recent work has shown that the interplay between short and long range connectivities in the Hopfield model leads to a deformation of the phase diagram with the appearance of novel phases [29]. It would be interesting to introduce short and long range connections in our model, and to examine how the coding efficiency of output neurons depends on the interaction between short and long range connections. This will be the object of future investigations.

### **Acknowledgements**

We have enjoyed extensive discussions with Inés Samengo and Elka Korutcheva. Valeria Del Prete thanks Isaac Perez-Castillo for very useful comments. Partial support from Human Frontier Science Programme grant RG 0110/1998-B.

- 
- [1] V. D. Prete, O. Steinberg, A. Treves, and E. Vaadia, to be submitted (2001).
  - [2] C. E. Shannon, AT&T Bell laboratories Technical journal **27**, 379 (1948).
  - [3] J. P. Nadal and N. Parga, Network **4**(3), 295 (1993).
  - [4] E. Korutcheva, J. P. Nadal, and N. Parga, Network **8**, 405 (1997).
  - [5] A. Turiel, E. Korutcheva, and N. Parga, J. Phys.A: Math. Gen. **32**, 1875 (1999).
  - [6] A. Campa, P. Del Giudice, N. Parga, and J. Nadal, Network **6**, 449 (1995).

- [7] J. P. Nadal and N. Parga, *Network* **4**, 295 (1994).
- [8] E. Korutcheva, V. D. Prete, and J. Nadal, *International Journal of Modern Physics B* **15**(3), 281 (2001).
- [9] E. T. Rolls and A. Treves, *Neural Networks and Brain Function* (Oxford University Press, Oxford, 1998).
- [10] W. Bialek, F. Rieke, R. R. de Ruyter van Steveninck, and D. Warland, *Science* **252**, 1854 (1991).
- [11] F. Rieke, D. Warland, R. R. de Ruyter van Steveninck, and W. Bialek, *Spikes: exploring the neural code* (MIT Press, Cambridge MA, 1996).
- [12] A. Treves, in *Neuro-informatics and Neural Modelling*, edited by F. Moss and S. Gielen (Elsevier, Amsterdam, 2000), vol. 4 of *Handbook of Biological Physics*, pp. 803–829.
- [13] V. D. Prete and A. Treves, *Phys. Rev. E* **64**, art.021912 (2001).
- [14] A. Treves, *J. Comp. Neurosci.* **2**, 259 (1995).
- [15] I. Samengo and A. Treves, *Physical Review E* **63**, art. 011910 (2001).
- [16] K. Kang and H. Sompolinsky, cond-mat/0101161 (2001).
- [17] A. Treves and E. Rolls, *Hippocampus* **2**(2), 189 (1992).
- [18] A. Treves, S. Panzeri, E. T. Rolls, M. C. A. Booth, and E. A. Wakeman, *Neural Comp.* **11**, 601 (1999).
- [19] M. Mezard, G. Parisi, and M. Virasoro, *Spin glass theory and beyond* (World Scientific Publishing Co Pte Ltd., Singapore, 1987).
- [20] D. J. Amit, *Modeling Brain Function* (Cambridge University Press, Cambridge, 1989).

- [21] A. Treves, J. Phys.A: Math. Gen. **23**, 2631 (1990).
- [22] S. Schultz and A. Treves, Physical Review E **57**(3), 3302 (1998).
- [23] A. Treves, Physical Review A **742**, 2418 (1990).
- [24] I. Perez-Castillo and V. D. Prete, in preparation (2001).
- [25] S. Panzeri, G. Biella, E. T. Rolls, W. E. Skaggs, and A. Treves, Network **7**, 365 (1996a).
- [26] E. T. Rolls, A. Treves, and M. J. Tovée, Exp. Brain Res. **114**, 149 (1997).
- [27] I. Samengo, to be published in Neural Computation (2001), cond-mat/0110074.
- [28] I. Perez-Castillo and V. D. Prete, in preparation (2001).
- [29] N. Skantzos and A. Coolen, J. Phys.A: Math. Gen. **34**, 929 (2001).